JOURNAL OF Applied Polymer SCIENCE

Composite Fibers from Poly(vinyl Alcohol) and Poly(vinyl Alcohol)-functionalized Multiwalled Carbon Nanotubes

Changfei Fu, Lixia Gu
State Key Laboratory for Modification of Chemical Fibers and Polymer Materials, College of Material Science and Engineering, Donghua University, Shanghai 201620, People's Republic of China
Correspondence to: L. Gu (E-mail: gulx@dhu.edu.cn)

ABSTRACT: High-strength composite fibers were prepared from poly(vinyl alcohol) (PVA) and multiwalled carbon nanotubes (MWNTs) functionalized with PVA matrix. Esterification between MWNTs and PVA was confirmed by Fourier transform infrared, Raman spectroscopy, thermogravimetric analysis, transmission electron microscope, and atomic force microscope. Homogeneous dispersion of PVA-functionalized MWNTs in dimethyl sulfoxide was affirmed by optical micrographs and particle size analysis. The PVA-functionalized MWNTs/PVA (1 wt %) composite fibers prepared by gel spinning and hot-drawing process exhibited tensile strength and modulus as high as 2.1 and 34 GPa, respectively, showing a 75% increase in tensile strength and 35% increase in modulus compared with pure PVA fibers. The mechanical properties were also much higher than untreated MWNTs/PVA (1 wt %) composite fibers and carboxylated MWNTs/PVA (1 wt %) composite fibers. From wide-angle X-ray diffraction, scanning electron microscopy, and Raman spectra analysis, higher mechanical properties of PVA-functionalized MWNTs/PVA composite fibers are attributable to homogeneous dispersion of MWNTs in PVA matrix, stronger interfacial adhesion between MWNTs and PVA matrix, and uniaxial orientation of MWNTs along fiber axis. © 2012 Wiley Periodicals, Inc. J. Appl. Polym. Sci. 000: 000–000, 2012

KEYWORDS: MWNTs; PVA; composite fibers; esterification; gel spinning

Received 5 May 2012; accepted 24 June 2012; published online
DOI: 10.1002/app.38260

INTRODUCTION

Carbon nanotubes (CNTs) as a reinforcing phase in the hosting polymer matrix have received much attention since their discovery in 1991[1] because of their unprecedented physical properties. Compared with conventional pseudo one-dimensional (1D) fillers such as alumina, glass, boron, silicon carbide, and carbon fiber, CNTs have a much higher specific surface, aspect ratio, and especially higher mechanical properties. The Young's modulus and tensile strengths of CNTs can be considered as high as 1 TPa[2] and 63 GPa,[3] respectively. A number of CNTs/polymer composites, such as poly(*p*-phenylene benzobisoxaole),[4] polyacrylonitrile,[5] polyimide,[6] with improved mechanical properties have been investigated. However, to make the most of the exceptional mechanical properties of CNTs, a large amount of work still needs to be done.

There are three predominant factors determining effective reinforcement of CNTs including homogeneous dispersion of CNTs in the host polymer matrix, stronger interfacial adhesion between CNTs and the matrix, and uniaxial or biaxial orientation of CNTs.

Noncovalent functionalization of CNTs using surfactants,[7,8] polyvinylpyrrolidone,[9,10] has been adopted to achieve the homogeneous dispersion of CNTs in the polymer matrix. However, noncovalently functionalized CNTs play a limited reinforcement role because the CNTs could only bonded with the matrix through weak interactions such as electrostatic, hydrophobic, or van der Waals forces, and the remaining of the dispersing agents in the polymer matrix will also influence the final mechanical properties of the composite. Therefore, many researchers have focused on covalently functionalized CNTs. Covalently bonded CNTs with the polymer matrix might be an ideal way to improve compatibility and load transfer ability between nanotubes and matrix. One really impressive demonstration of covalently functionalized CNTs has been made by Sun and coworkers[11,12] for preparing poly(vinyl alcohol) (PVA)/single-walled carbon nanotubes (SWNTs) composite films where great care has been taken to achieve good dispersion and strong interfacial adhesion. They solubilized SWNTs through the covalent attachment of PVA and then dispersed the PVA-functionalized SWNTs into the PVA matrix for the fabrication of composite films via a wet-casting method. Alignment of CNTs can be achieved through shearing,[13,14] magnetic field,[15,16] or mechanical stretching.[17,18] Fibers can be easily drawn, and CNTs were preferred to form orientation parallel to the fiber axis. Poulin and

coworkers[19] treated wet-spun composite fibers made of CNTs and PVA through a hot-drawing process to achieve high toughness and alignment.

PVA is widely used as matrix polymer for thin films or fibers. PVA/CNTs composite fibers were successfully processed using solution spinning,[20,21] gel spinning,[22–24] or electrospinning[25] technology. Our research focused on preparation and characterization of composite fibers by gel spinning and hot-drawing process from PVA and multiwalled carbon nanotubes (MWNTs) covalently functionalized with the matrix polymer. For comparison, four kinds of fibers including: the pure PVA fibers, the untreated MWNTs/PVA composite fibers, the carboxylated MWNTs/PVA composite fibers, and the PVA-functionalized MWNTs/PVA composite fibers were prepared. This article is mainly focus on the improvement of the mechanical properties by the homogeneous dispersion, strong interfacial bonding, and effective orientation of PVA-functionalized MWNTs in PVA fibers.

EXPERIMENTAL

Materials

MWNTs produced by a catalyzed chemical vapor deposition process were purchased from Shenzhen Nanotech Port (Shanghai, China) with 5% of carbon impurities and catalysts, and the length of MWNTs is in the range of 0.5–5 μm and diameter of 10–30 nm. PVA, with degree of polymerization (DP) of 1700 and degree of hydrolysis of 99%, was supplied by Sinopec Shanghai Petrochemical (Shanghai, China). *N*, *N*′-dicyclohexylcarbodiimide (DCC, 99%), dimethyl sulfoxide (DMSO, 99.5%), 4-(dimethylamino) pyridine (DMAP, 99%), nitric acid (65%), sulfuric acid (98%), and ethanol were obtained from Sinopharm Chemical Reagent. 1-hydroxybenzotriazole (HOBT, 99%) and dialysis tubing (cut-off molecular weight $\sim$ 100 000 and $\sim$ 14,000) were purchased from Yuanju Bio-tech (Shanghai, China).

Functionalization of MWNTs

Functionalization of MWNTs with PVA through esterification was reported by Sun and coworkers.[11] Initially, the 500 mg MWNTs were subjected to strong acid treatment using 83 mL sulfuric acid (98%) and 133 mL nitric acid (65%). The carboxylated MWNTs from acid treated MWNTs were produced by heating under reflux for 1 h followed by centrifuging, dialysis against fresh deionized water, and drying under vacuum. The esterification was achieved by functionlizing of carboxylated MWNTs with PVA through carbodiimide-activated esterification. DCC (1000 mg), DMAP (165 mg), HOBT (325 mg), and carboxylated MWNTs (490 mg) were dissolved in 50 mL DMSO, followed by sonication in Shumei KQ2200DB bath sonicator for 1 h (frequency 40 kHz, power 100 W, sonication bath temperature was maintained 20–30°C by using continuous coldwater flow in the bath). Then, a solution of PVA in DMSO (21 mg/mL, 10 mL) was added and the mixture was sonicated on the same sonicating condition of frequency, power, and temperature for another 24 h. The obtained dark suspension was centrifuged to remove the solid residue and washed with acetone after evaporating the DMSO. After that, the suspension was dissolved in hot water and placed in dialysis tubing for dialysis against fresh deionized water. Finally, the PVA-functionalized MWNTs were obtained after vacuum dried.

Preparation of PVA-Functionalized MWNTs/PVA Composite Fibers

Gel spinning and hot-drawing process were adopted to prepare PVA-functionalized MWNTs/PVA composite fibers. PVA-functionalized MWNTs (150 mg) were dispersed in 77.3 mL DMSO. Meanwhile, 14.85 g PVA was added into this dispersion followed by stirring and sonication in Shumei KQ2200DB bath sonicator (frequency 40 kHz, power 100 W, and bath temperature 95°C) for 4 h. The optically homogeneous PVA-functionalized MWNTs/PVA solution was obtained.

Gel spinning was performed by extruding the PVA-functionalized MWNTs/PVA solution from a spinneret having diameter of 0.8 mm. The solution kept at 70°C was extruded into open air through an air gap of 10 mm, between spinneret and coagulating bath, and then immediately coagulated in ethanol at −5°C to obtain as-spun fibers. Then, the as-spun fibers were drawn in hot air by two steps, first at 150°C (draw ratio = 3) and second 180°C (draw ratio = 3), respectively. PVA-functionalized MWNTs/PVA composite fibers were obtained.

For comparison, pure PVA fibers, the untreated MWNTs/PVA composite fibers, and the carboxylated MWNTs/PVA composite fibers were also prepared using the same procedures described above.

Measurement and Characterization

Fourier transform infrared (FTIR) spectra were obtained using Nicolet 8700 IR spectrometer. All the spectra were collected in transmittance through KBr pellet. Raman spectra of PVA, untreated MWNTs, carboxylated MWNTs, PVA-functionalized MWNTs, and composite fibers were recorded with a Renishaw inVia Reflex micro-Raman spectrometer with 514-nm laser excitation. For polarized Raman spectra, the fiber was rotated 90°, so that the direction of the E-vector of the polarized laser light was parallel and perpendicular oriented to the fiber axis. Thermogravimetric analysis (TGA) measurements were performed with a Perkin Elmer TGA7 instrument at a heating rate of 20°C/min from 35 to 700°C under a nitrogen atmosphere. Transmission electron microscope (TEM) were performed on a JEOL JEM-2010 TEM. Atomic force microscope (AFM) images were obtained using a Veeco NanoScope IV AFM in tapping mode. Optical micrographs were obtained with polarizing optical microscopy (POM, BX51 Olympus). The particle size distributions of different MWNTs in DMSO were obtained using JL 9200 Static Light Scattering Particle Size Analyzers. Tensile measurements were carried out by a DXLL-20000 tensile tester, the fiber length was 150 mm and a tensile speed of 100 mm/min was used. Wide-angle X-ray diffraction (WAXD) was used to determine the crystallinity and crystal orientation of the fibers. The morphological structure of the cross section of as-spun fibers and profiles parallel to the fiber axis of the drawn fibers was observed using Hitachi S-3000 scanning electron microscope (SEM) made in Japan after sputter coating the samples with gold.

RESULTS AND DISCUSSION

Functionalization of MWNTs

It is now well known that CNTs can be carboxylated after treating with strong acids mixture.[26] These strong acids as oxidizing

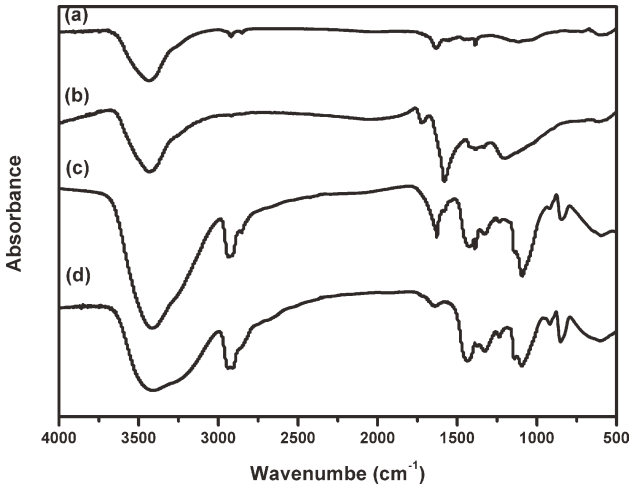

Figure 1. FTIR spectra of (a) untreated MWNTs, (b) carboxylated MWNTs, (c) PVA-functionalized MWNTs, and (d) pure PVA.

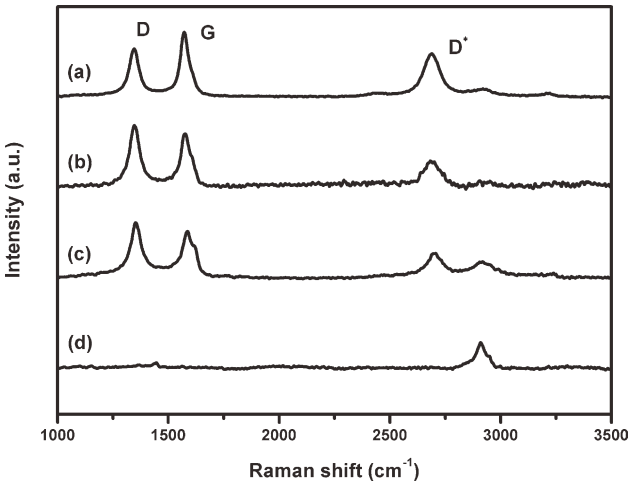

Figure 2. Raman spectra of (a) untreated MWNTs, (b) carboxylated MWNTs, (c) PVA-functionalized MWNTs, and (d) pure PVA.

reagents remove the caps of the CNTs and introduce defects involving oxygen functionalities, which mainly in the forms of carboxylic acid groups on the surface and the ends of CNTs. These carboxylic acid groups are expected to react with pendant hydroxyl groups of PVA by esterification.[11] FTIR spectra were used to identify the carboxylation reactions and the ensuing esterification. Figure 1(a–d) shows FTIR spectra of untreated MWNTs, carboxylated MWNTs, PVA-functionalized MWNTs, and pure PVA, respectively. In Figure 1(a), the absorption peak at 1632 cm^{-1} corresponds to C=C double bonds of untreated MWNTs. The following FTIR data of carboxylated MWNTs [Figure 1(b)] clearly indicate that carboxylic acid groups have been successfully introduced into MWNTs: 1723 cm^{-1} (C=O stretching vibration), 1580 cm^{-1} (COO^- asymmetrical stretching vibration), 1392 cm^{-1} (COO^- symmetrical stretching vibration), 1212 cm^{-1}(C—O stretching vibration). Although pure PVA was partially acetylated (degree of hydrolysis of 99%), carbonyl stretching vibration absorption peak was not found in Figure 1(d). Compared with carboxylated MWNTs, the carbonyl stretching frequency of PVA-functionalized MWNT [Figure 1(c)] has shifts to a lower frequency (1709 cm^{-1}) because of conjugated effect of carbonyls of ester linkages and fullerenes of MWNTs, and the absorption peak around 1083 cm^{-1} is associated with the C—O—C stretching vibration. The existence of ester groups indicates that PVA chains have been successfully grafted onto MWNTs.

More evidence for the carboxylation reaction and the esterification was obtained by Raman spectroscopy, which is a powerful tool used to characterize functionalization of CNTs. As shown in Figure 2, the Raman spectra of untreated MWNTs, carboxylated MWNTs, and PVA-functionalized MWNTs exhibit the characteristic peaks of MWNTs, namely the D-band at 1343–1354 cm^{-1}, the G-band at 1571–1587 cm^{-1}, and the D*-band at 2682–2708 cm^{-1}, which attributed to the defects and disorder-induced peaks, tangential-mode peaks, and a second harmonic of the D-band, respectively. Typically, the relative intensity between the D-band and the G-band (I_D/I_G) is frequently used to assess the degree of structural disorder in MWNTs samples. The intensity ratio I_D/I_G for carboxylated MWNTs is 1.15, which is greater than that of untreated MWNTs (0.74). This indicates a partial destruction of the conjugation structure of MWNTs as a result of the increase of the amount of sp^3-hybridized carbons. The ratio I_D/I_G for PVA-functionalized MWNTs (1.19) increases slightly compared with that of carboxylated MWNTs (1.15), indicating that esterification has no important effect on the degree of structural disorder of the nanotubes.

Based on TGA analyses (Figure 3), the PVA content trapped in PVA-functionalized MWNTs was estimated in terms of mass balance calculations from the residual weight at 700°C of neat PVA (1.3 wt %), carboxylated MWNTs (88.9 wt %), and PVA-functionalized MWNTs (63.1 wt %), it was about 29.4 wt %, approximately corresponding to rate of charge (the mass ratio of carboxylated MWNTs and neat PVA was 7 : 3) in esterification stage. As observed in Figure 3, at lower temperature stages below 200°C, weight loss could be attributed to the loss of solvent and initial volatile degradation products. At higher

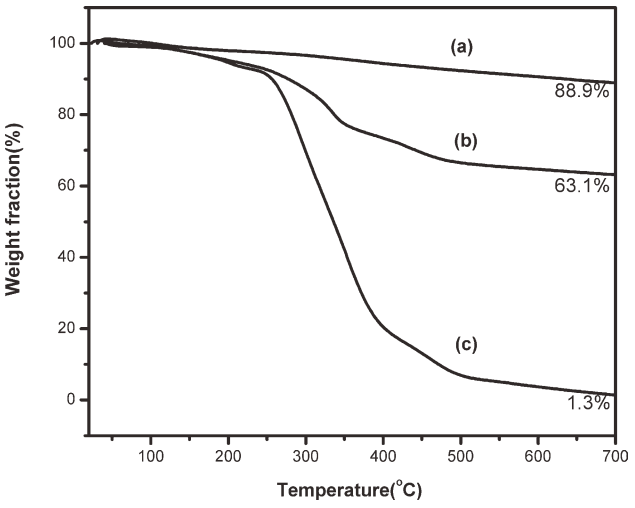

Figure 3. TGA diagrams of (a) carboxylated MWNTs, (b) PVA-functionalized MWNTs, and (c) pure PVA.

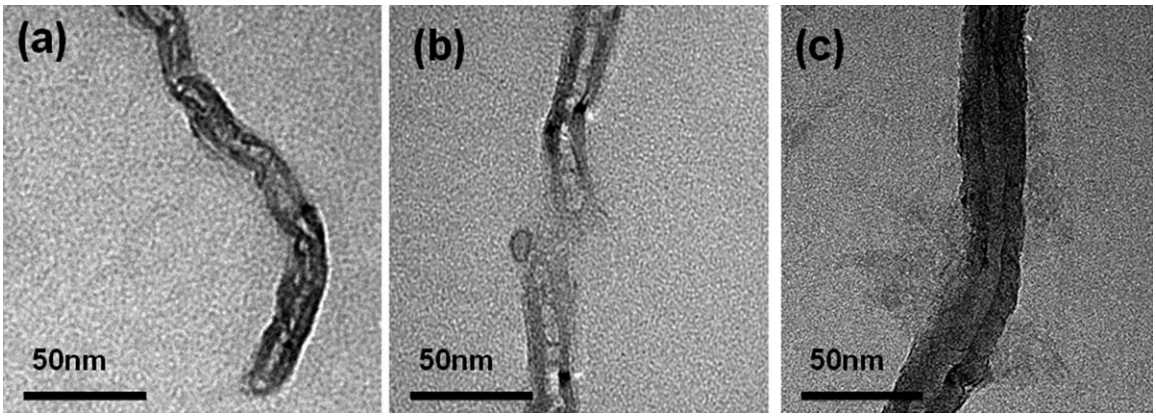

Figure 4. TEM images of (a) untreated MWNTs; (b) carboxylated MWNTs; and (c) PVA-functionalized MWNTs.

temperature stage, two weight loss steps could be observed from the TGA curves of both pure PVA and PVA-functionalized MWNTs, which were attributed to the decomposition of the side chain and backbone of the polymer, respectively.[27,28] The first weight loss step corresponding to dehydration and de-esterification reaction on the polymer side chain, the onset of the thermal degradation temperature of pure PVA was at 250°C, and the onset temperature of PVA-functionalized MWNTs was shifted slightly to higher temperature at 260°C. This should be due to restriction of mobility of polymer chain and suppression of the decomposition in PVA-functionalized MWNTs. The second decomposition step was associated with the polyene residues degradation which yields carbon and hydrocarbons. The decomposition of the backbone of PVA in PVA-functionalized MWNTs began at around 415°C, and it in pure PVA began at around 430°C. This indicates that MWNTs exhibit a good thermal transfer capability.

Typical TEM images of untreated MWNTs, carboxylated MWNTs, and PVA-functionalized MWNTs show the morphology changes of MWNTs after acid treatment and esterification (Figure 4). It is clear that the untreated MWNTs had closed tubular structures [Figure 4(a)], while the caps of MWNTs were removed after acid treatment [Figure 4(b)]. This is mainly because that during the acid treatment, oxidation were occurred at defect sites and caps on nanotubes, therefore the tubes might be cut into pieces and the caps of MWNTs were removed. After esterification, a polymer layer was wrapped on the surface of MWNTs, which made the diameter of PVA-functionalized MWNTs was about 10 nm thicker than that of untreated MWNTs and carboxylated MWNTs. The diameters of PVA-functionalized MWNTs were at around 25 nm [Figure 4(c)], while the diameters of untreated MWNTs and carboxylated MWNTs were both at about 15 nm. The carboxyl groups on MWNTs were generated from the oxidation of defect site on MWNTs; they were not homogenously distributed on the surface of MWNTs, therefore the polymers were not evenly coated on the surface of MWNTs after esterification.

Figure 5 shows the tapping mode 2D (left) and 3D (right) AFM height images of individual CNT of various samples. It is obvious that the untreated MWNTs had a relatively prefect structure [Figure 5(a)], while after acid treatment, the defects on MWNTs were increased and the tubular structure of MWNTs became irregular [Figure 5(b)]. Also, from Figure 5(c), it can be seen that the individual nanotube had different heights at different locations on the tube, indicating that not all of the tube surfaces were covered evenly by the layer which preferred coating defect sites and the endpoints on MWNTs. The AFM observations were consistent with the TEM results. Combined with all analysis above, it can be inferred that the coated layer on the surface of PVA-functionalized MWNTs were PVA macromolecular chains.

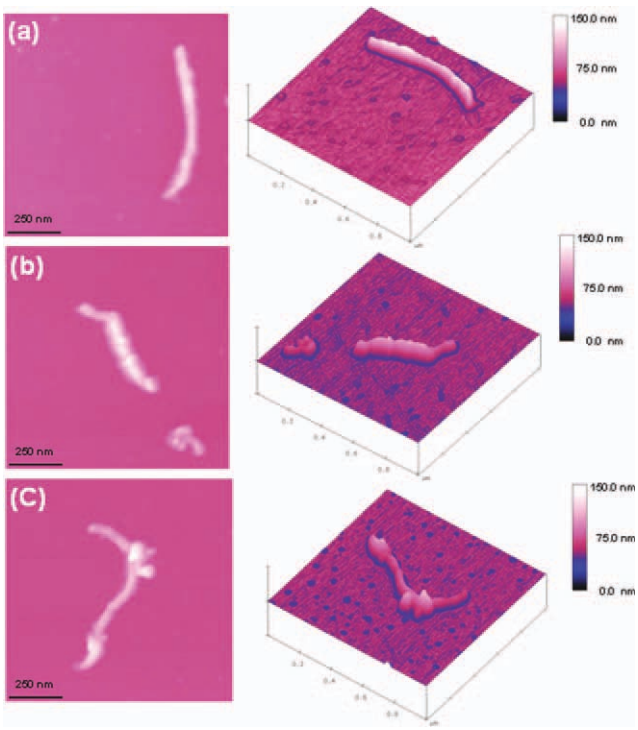

Figure 5. AFM height images of (a) untreated MWNTs; (b) carboxylated MWNTs; and (c) PVA-functionalized MWNTs. [Color figure can be viewed in the online issue, which is available at wileyonlinelibrary.com.]

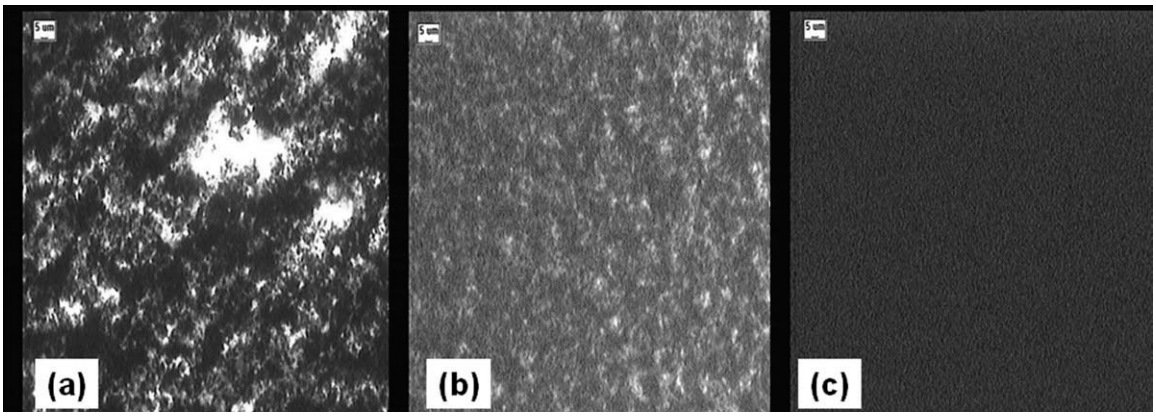

Figure 6. Polarized optical images of (a) untreated MWNTs; (b) carboxylated MWNTs; (c) PVA-functionalized MWNTs in DMSO solvent (150 mg MWNTs in 77.3 mL DMSO).

Dispersion of Functionalized MWNTs in DMSO Solvent

The dispersibility of MWNTs can be improved after surface modification. As shown in Figure 6, untreated MWNTs formed large agglomeration in DMSO solvent, the acid-treated MWNTs showed a better dispersibility, but still some aggregates were exist in the dispersion. While in PVA-functionalized MWNTs/DMSO dispersion, there could barely see the existence of large particles, indicating that the PVA-functionalized MWNTs had much better dispersibility than untreated MWNTs and carboxylated MWNTs. The untreated MWNTs had relative smooth surface, small diameter, large surface area, and strong Van der Waals force, therefore the tubes were easily form entanglement structure. After acid treatment, the carboxyl groups were introduced on the surface of MWNTs, the sulfoxide groups in DMSO molecule could form strong hydrogen bonds with carboxyl groups (S═O…HO─C═O), thus improved the dispersion of carboxylated MWNTs in DMSO solvent. However, the amount of ─COOH groups which were introduced on the surface of MWNTs were quite small; the agglomerations were still easily occur. After esterification, as a large amount of PVA macromolecular chains were grafted to the surface of MWNTs, PVA chain segments which had a large number of hydroxyl groups could form strong hydrogen bonds with sulfoxide groups from DMSO molecules (S═O…HO), this ensured PVA-functionalized MWNTs easily form uniform dispersion in DMSO solvent. The dispersion of PVA-functionalized MWNTs in DMSO solvent was stable for several weeks without visible phase separation, while untreated MWNTs and carboxylated MWNTs were settled at the same conditions.

The particle size distributions of different MWNTs dispersed in DMSO were shown in Figure 7. The untreated MWNTs could not form homogeneous dispersion in DMSO; therefore, there particle size distribution in DMSO could not be measured. The *Z*-average diameter of carboxylated MWNTs and PVA-functionalized MWNTs were 199.8 and 403.9 nm, respectively. The larger diameter of PVA-functionalized MWNTs was mainly due to the coated PVA layers on the surface of MWNTs which were formed through esterification.

Characterization of MWNTs/PVA Composite Fibers

PVA-functionalized MWNTs/PVA fiber was prepared by the gel spinning process. The fiber extruded from the spinning solution was firstly stayed in the air for a while and then immersed into the low-temperature coagulation bath to form gel fiber. Keller[29] has pointed out that the polymer solution usually tends to generate tassel-like microcell nuclei at the large degree of cooling, while the small degree of cooling mainly induces the polymer to produce folded chain lamellae. As-prepared gel fiber has a uniform microporous network gel structure which contains a lot of sprouts-like microcellular nuclei. The gel structure minimizes chain entanglements and ensures polymer orientation under drawing, the microcellular nuclei act as physical crosslinks to prevent chain slipping and induces polymer crystallization. Both PVA-functionalized MWNTs/PVA and carboxylated MWNTs/PVA spinning solutions showed excellent spinning ability and their as-spun fibers exhibited good drawing ability. However, untreated MWNTs could block the spinneret even with higher pressure. To understand the impact of PVA-functionalized MWNTs on the composite fibers, the untreated MWNTs/PVA, carboxylated MWNTs/PVA composite fibers, and pure PVA fibers were adopted same process parameters with PVA-functionalized MWNTs/PVA composite fibers. For instance, PVA solution concentration, MWNTs addition amount (1 wt %), injection speed, take-up speed, coagulation bath temperature, first heat treatment temperature, second heat treat temperature and draw ratio, and so forth.

The mechanical properties of pure PVA and MWNTs/ PVA composite fibers were shown in Table I, and Figure 8 shows typical stress–strain curves for the various drawn fibers. Although the shapes of the stress–strain curve for all of fibers

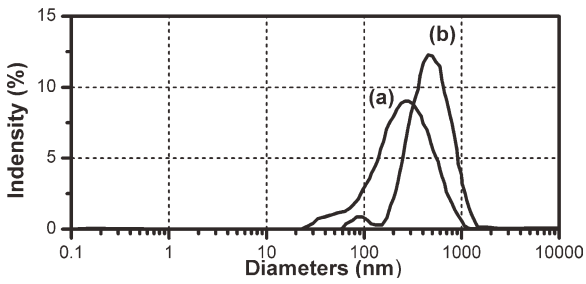

Figure 7. Size distribution of (a) carboxylated MWNTs and (b) PVA-functionalized MWNTs in DMSO solvent.

Table I. Mechanical Properties of the Drawn Fibers

Sample	Diameter (μm)	Tensile strength (GPa)	Modulus (GPa)	Elongation (%)
Pure PVA fibers	44.3 ± 1.6	1.2 ± 0.1	25.2 ± 2.5	10.5± 0.3
Untreated MWNTs/PVA fibers	45.6 ± 4.0	1.5 ± 0.2	29.5 ± 3.2	10.0 ± 1.6
Carboxylated MWNTs/PVA fibers	45.5 ± 2.3	1.7 ± 0.1	30.4 ± 3.0	10.3 ± 1.0
PVA-functionalized MWNTs/PVA fibers	44.5 ± 2.5	2.1 ± 0.1	34.1 ± 3.0	11.7 ± 1.0

were similar, the yield points and break points of three kinds of composite fibers were significantly higher than that of pure PVA fibers. Especially, the tensile strength and Young's modulus of PVA-functionalized MWNTs/PVA composite fibers were extraordinarily improved compared with pure PVA fibers by around 75 and 35%, respectively. It is noticed that the tensile strength and modulus of PVA-functionalized MWNTs/ PVA composite fibers were considerably increased in comparison with untreated MWNTs/PVA composite fibers and carboxylated-MWNTs/PVA composite fibers. This result indicated that the reinforce effect of PVA-functionalized MWNTs was much better than untreated MWNTs and carboxylated MWNTs.

To understand the reason for the enhancement of mechanical properties, the WAXD analysis was used to investigate the crystal structure of pure PVA and MWNTs/PVA composite fibers. The WAXD patterns were shown in Figure 9. The figure shows the WAXD patterns of MWNTs /PVA composite fibers still keep the characteristic peaks of pure PVA, indicating that incorporation of MWNTs did not significantly affect the crystalline structure. However, because of the low content of MWNTs (1 wt %) in the composites combined with the curved structure of nanotubes, the reflection assigned to the (002) peak of the hexagonal graphite structure (layer spacing within the MWNT) at 26° was not clearly seen in the WAXD patterns of the composite fibers.

Table II lists the crystallite size, crystallinity, and crystallite orientation of PVA in pure PVA and MWNTs /PVA composite fibers. The change in crystallite size determined from WAXD using Scherrer's equation for the various drawn fibers was considered within experimental error. The degrees of crystallite orientation for the PVA component in various fibers were very similar. The crystallinity of PVA in PVA-functionalized MWNTs/PVA composite fibers were significantly increased compared with other fibers indicating that the PVA-functionalized MWNTs were act as nuclear sites and promoted the heterogeneous nucleation process of PVA. It could be inferred that as PVA molecular chains grafted to MWNTs, PVA-functionalized MWNTs in gel network of as-spun fibers not only acted as physical crosslink to help drawing, but served on template to induce PVA crystallization during hot drawing. The PVA chains which were grafted on MWNTs could be also assemble into lattice, resulting in the effective load transfer and improved the strength and modulus of the fibers.

The good dispersion of MWNTs in PVA matrix is also one of important reasons of high tensile strength and high modulus for MWNTs-reinforced composite fibers. However, it remains a challenge because of the strong van der Waals interactions among MWNTs. To investigate dispersion of MWNTs in PVA matrix, TEM was used to observe the cross-section morphology of as-spun fibers. Figure 10 shows the SEM micrographs of the cross section of the four kinds of as-pun fibers. PVA-functionalized MWNTs were well dispersed in PVA matrix [Figure 10(d)],

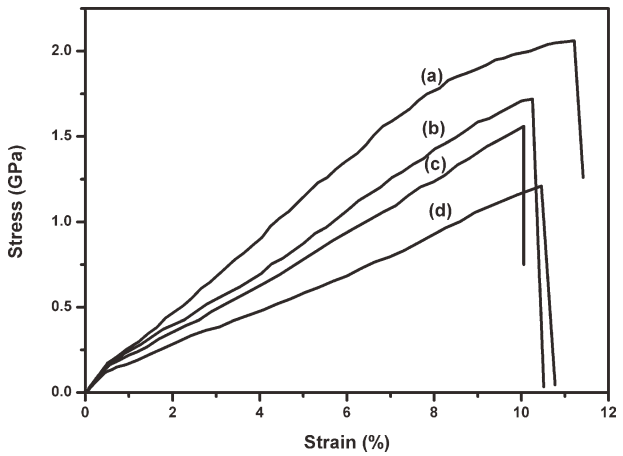

Figure 8. Stress–strain curves of (a) PVA-functionalized MWNTs/PVA; (b) carboxylated MWNTs/PVA; (c) untreated MWNTs/PVA, and (d) pure PVA fibers.

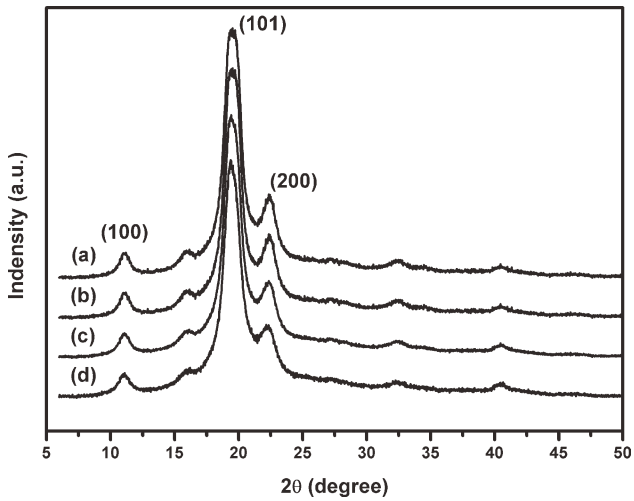

Figure 9. WAXD diffractograms of (a) PVA-functionalized MWNTs/PVA; (b) carboxylated MWNTs/PVA; (c) untreated MWNTs/PVA, and (d) pure PVA fibers.

Table II. Structural Parameters of the Drawn Fibers

	Crystal size for various fibers (nm)			
Miller index (hkl)	PVA	Untreated MWNTs/PVA	Carboxylated MWNTs/PVA	PVA-functionalized MWNTs/PVA
(100)	7.5	7.8	7.6	7.2
(101)	6.4	6.2	6.7	6.2
(200)	6.1	6.3	5.9	5.9
Crystallinity (%)	62.9	63.3	65.4	69.2
Crystallite orientation	92.8	91.7	92.4	92.8

while some agglomerates were observed in untreated MWNTs/PVA fibers [Figure 10(b) circled place]. Although carboxylated-MWNTs shown a slightly better dispersion state in PVA matrix compared with untreated MWNTs, there were still some MWNTs aggregates existed in the fiber [Figure 10(c) circled place]. Thus, homogeneous dispersion of PVA-functionalized MWNTs is attributable to the covalently bonded PVA molecule chains on the surface of MWNTs, which ensure homogeneous dispersion in spinning solution. Another notable phenomenon observed through TEM micrographs is that some MWNTs were exposed outside the PVA matrix for untreated MWNTs/ PVA composite fibers [Figure 10(b) arrows point place], indicating that interfaces adhesion between untreated MWNTs and PVA matrix was weak and nanotubes were easily pulled out from PVA matrix when the fiber was fractured. It could be speculated that MWNTs would slip and the load could not be effectively transferred when untreated MWNTs/PVA fibers were fractured. For PVA-functionalized MWNTs, the covalent bonded PVA chains on the surface of MWNTs have very good compatibility with PVA matrix, leading to strong interfaces adhesion between MWNTs and PVA matrix.

To reveal the internal fiber structure, the drawn fibers were split by using a needle for SEM observation. Figure 11 shows the SEM images of profiles parallel to the fiber axis of different

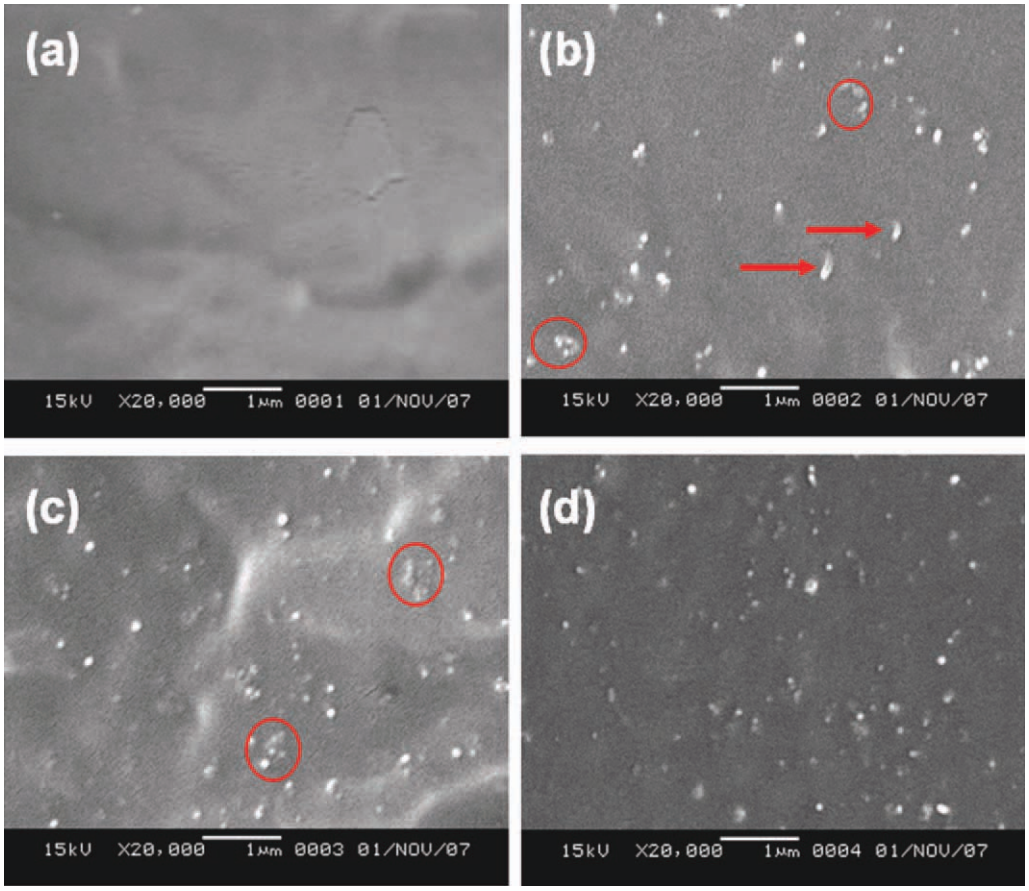

Figure 10. SEM micrographs of the fractured surfaces of the as-spun (a) PVA; (b) untreated MWNTs/PVA; (c) carboxylated MWNTs/PVA, and (d) PVA-functionalized MWNTs/PVA fibers. [Color figure can be viewed in the online issue, which is available at wileyonlinelibrary.com.]

Applied Polymer SCIENCE

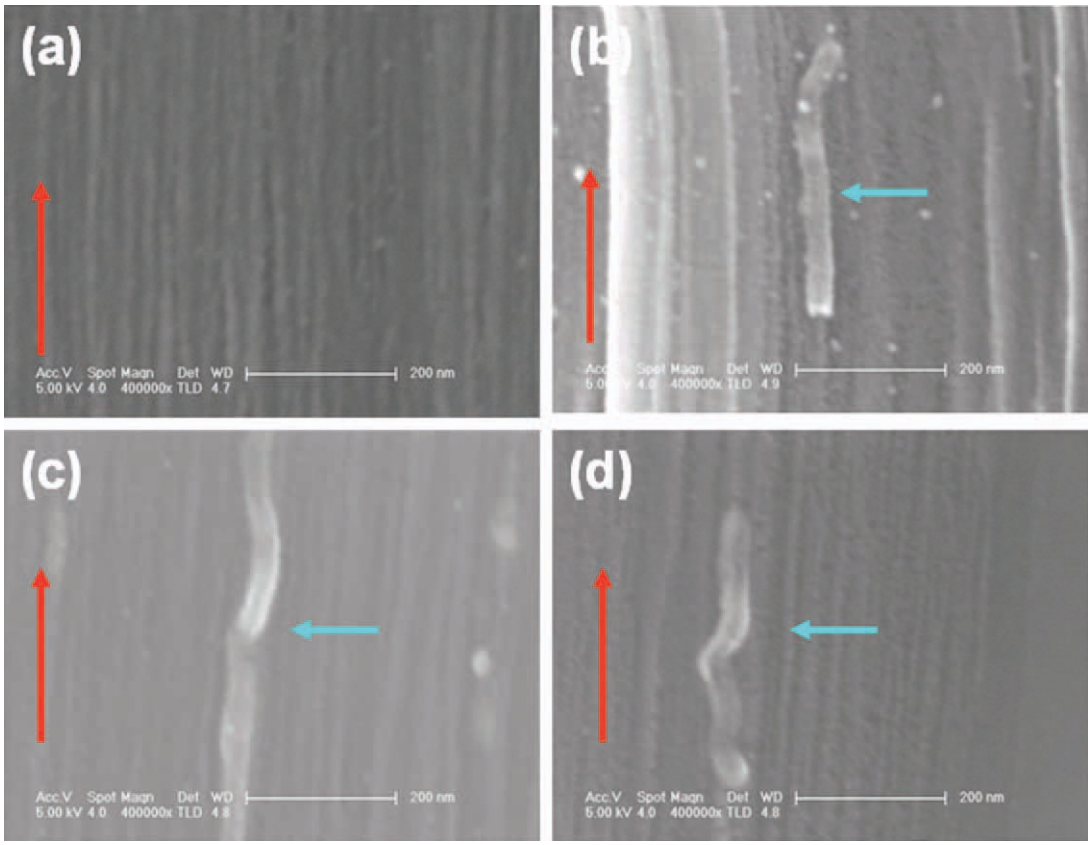

Figure 11. SEM micrographs of profiles parallel to the fiber axis of the drawn (a) PVA; (b) untreated MWNTs/PVA; (c) carboxylated MWNTs/PVA, and (d) PVA-functionalized MWNTs/PVA fibers. [Color figure can be viewed in the online issue, which is available at wileyonlinelibrary.com.]

drawn fibers. Vertical arrow points the direction of fiber axis. It can be clearly seen that there were many fibrils with diameters around 30 nm arranged parallel to the fiber axis. Horizontal arrow points MWNTs. It is obvious that untreated MWNTs, carboxylated MWNTs, and PVA-functionalized MWNTs were orientated along the fiber axis and parallel to the fibrils. The original curved MWNTs also showed a stretched morphology. It could be interpreted that the nozzle shear and the hot-drawing process ensured the orientation and stretching of MWNTs in PVA fiber matrix. The orientation and stretching of MWNTs in PVA matrix were considered the one of critical reasons for the enhancement of mechanical properties of composite fibers. From Figure 11(b), we can see that untreated MWNTs were peeled off from the PVA matrix, suggesting that there was the poor adhesion between untreated MWNTs and PVA matrix. Carboxylated-MWNTs show a better compatibility with PVA matrix, but there still some protrusion points were found [Figure 11(c)]. Both ends of PVA-functionalized MWNTs were embedded in the fibrils, the interface between MWNTs and PVA matrix was quite fuzzy [Figure 11(d)]. As better wetting with matrix judged from the SEM patterns, PVA-functionalized MWNTs can be expected to be more effective to improve the mechanical properties of composite fibers than other composite fibers. Also in profiles of untreated MWNTs/PVA composite fibers, some white spots were observed, these white spots were graphite impurities contained in the untreated MWNTs.

To further explore the interfacial interaction between matrix and MWNTs, Raman spectroscopy was used to characterize MWNTs in the drawn fibers. As shown in Figure 12, the D- and G-bands of MWNTs in the drawn fibers, attributed to the defects and disorder-induced modes and in-plane E_{2g} zone-

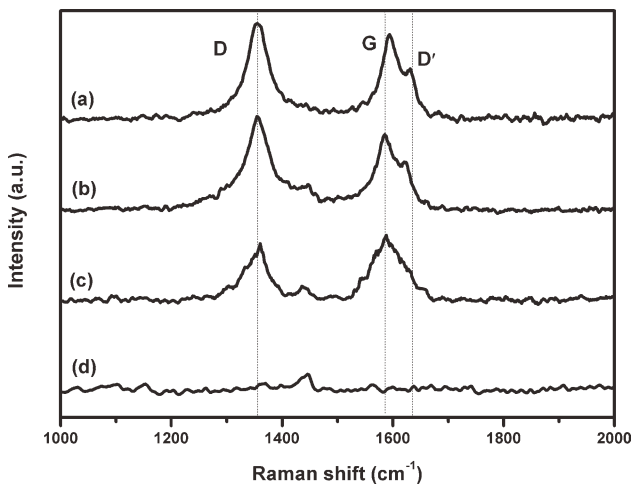

Figure 12. Raman spectra of (a) PVA-functionalized MWNTs/PVA, (b) carboxylated MWNTs/PVA, (c) untreated MWNTs/PVA composite fibers, and (d) pure PVA fibers.

center mode, are consistent with the Raman spectra of MWNTs samples shown in Figure 2. However, the D′-band of PVA-functionalized MWNTs and carboxylated MWNTs in the drawn fibers at about1625 cm^{-1}, which is known to be directly affected by the disorder in nanotubes, exhibits a difference with MWNTs samples in Figure 2, indicating an increase in defects along the tube body during spinning and drawing.[30] In addition, different with the previous reports on PVA-functionalized CNTs composites,[11,12] the peaks of the G-band of PVA-functionalized MWNTs/PVA composite fibers were shifted to the higher frequencies by about 8 cm^{-1} compared with that of untreated MWNTs/PVA, carboxylated MWNTs/PVA composite fibers, which suggests that the PVA-grafted MWNTs are completely different from MWNTs/PVA mixtures in terms of Raman characteristics. For PVA-functionalized MWNTs, PVA chain is individually anchored to the nanotubes surface, forming a nanoscale layer of coverage. This phenomenon exhibits that MWNTs were influenced by the covalent PVA environment. The upshift of the G-band for PVA-functionalized MWNTs in drawn composite fibers was attributed to charge transfer between MWNTs and PVA, implying interfacial affinity between them.

Raman spectroscopy can also provide information for orientation of MWNTs in PVA matrix. Fischer[31] investigated MWNT/polycarbonate composites and characterized the MWNTs orientation characterized more or less roughly be comparison of Raman spectra parallel and perpendicular to the fiber axis, and the relative intensity (I_D/I_D) of D bands parallel and perpendicular to the fiber axis, as well as the relative intensity (I_G/I_G) of G bands parallel and perpendicular to the fiber axis, was used to quantify the degree of orientation of the MWNTs in the composite fiber. Raman spectra parallel and perpendicular to the fiber axis of three kinds of drawn MWNTs/PVA composite fibers were shown in Figure 13. The intensity ratios (I_D/I_D) were 3.97, 3.98 and 4.02 for unteated MWNTs/PVA, carboxylated MWNTs/PVA and PVA-functionalized MWNTs/PVA composite fibers, respectively, and the intensity ratios (I_G/I_G) were 2.47, 2.46 and 2.50 for three kinds of fibers, respectively. First, the ratios were very large compared with isotropic composites (value = 1), indicating that the degree of orientation of MWNTs in composite fibers was very high. Second, the ratios for various composite fibers were almost identical. This can be explained with approximately the same alignment orientation of MWNTs in the composite fibers. So, we can conclude that the same spinning and hot-drawing process parameters lead to roughly the same degree of orientation of the MWNTs. Orientation of MWNTs parallel to the fiber axis is crucial for improved mechanical properties, so the three kinds of MWNTs exhibit extraordinary reinforcing efficiency. As the same degree of orientation of MWNTs, the better mechanical performance of PVA-functionalized MWNTs/PVA composite fibers is attributable to the better dispersion and the stronger covalent interfacial bonding between MWNTs and PVA matrix.

In this study, MWNTs and a commercial DP grade of PVA (DP: 1700) were used to fabricate PVA/CNTs composite fibers. For the purpose of higher strength and higher modulus, SWNTs seem to be more preferable compared to MWNTs, because of higher aspect ratio, higher mechanical properties, and possible higher load transfer. However, the prices for MWNTs are much lower than for SWNTs, and closer to commercial use. Although the highest strength of the PVA/CNTs composite was achieved at 2.6 GPa as reported in the literature,[24] SWNTs and the PVA with much higher molecular weight (DP: 18,000) were used. Our results show that enhancement of mechanical properties can be achieved by using PVA-functionalized MWNTs and a commercial DP grade of PVA (DP: 1700), which are beneficial for industrial scale production.

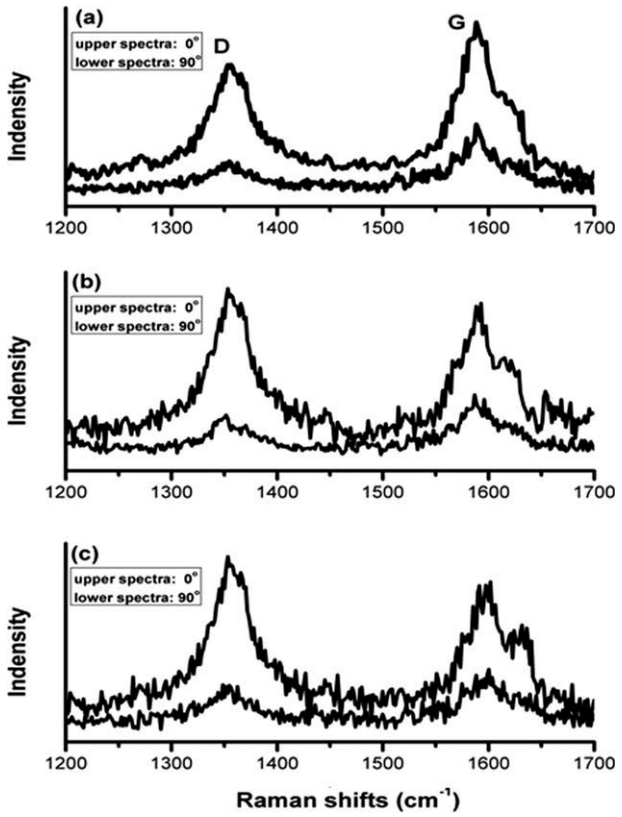

Figure 13. Raman spectra parallel and perpendicular to fiber axis of (a) untreated MWNTs/PVA, (b) carboxylated MWNTs/PVA, and(c) PVA-functionalized MWNTs/PVA composite fibers. Upper spectra: parallel to fiber axis; lower spectra: perpendicular to fiber axis.

CONCLUSIONS

MWNTs were functionalized with PVA through esterification reactions. FTIR, Raman spectroscopy, TGA, TEM, and AFM results showed that PVA chains were covalently bonded with MWNTs. Polarizing microscopy and particle size analysis showed that PVA-functionalized MWNTs could be homogeneously dispersed in the solvent DMSO. PVA-functionalized MWNTs/PVA composite fibers were prepared by gel spinning and hot drawing. PVA-functionalized MWNTs/PVA (1 wt %) composite fibers notably exhibit tensile strength and modulus as high as 2.1 GPa and 34 GPa, respectively, showing a 75% increase in tensile strength and 35% increase in modulus compared with pure PVA fibers. The mechanical properties of PVA-functionalized MWNTs/PVA (1 wt %) composite fibers were also much higher than untreated MWNTs/PVA (1 wt %)

composite fibers and carboxylated MWNTs/PVA (1 wt %) composite fibers. WAXD results showed that PVA-functionalized MWNTs could induce PVA molecular chains crystallization. SEM micrographs of cross section of as-pun fibers and profiles parallel to the fiber axis of the drawn fibers reveal PVA-functionalized MWNTs were homogeneously dispersed in the PVA matrix and orientated along fiber axis, the good compatibility between PVA-functionalized MWNTs and PVA matrix was also confirmed by TEM observation. Roman spectra analyses revealed interfacial affinity between PVA-functionalized MWNTs and PVA matrix. Raman spectra parallel and perpendicular to fiber axis revealed high degree of orientation of the MWNTs in the drawn composite fibers. Homogeneous dispersion of MWNTs in PVA matrix, stronger interfacial adhesion between MWNTs and the matrix, and uniaxial orientation of MWNTs corporately result in higher mechanical properties of PVA-functionalized MWNTs/PVA composite fibers.

REFERENCES

1. Iijima, S. *Nature* **1991,** *354*, 56.
2. Wong, E.W.; Sheehan, P. E.; Lieber, C. M. *Science* **1997,** *277*, 1971.
3. Yu, M.; Lourie, O.; Dyer, M. J.; Kelly, T.F.; Ruoff, R. S. *Science* **2000,** *287*, 637.
4. Kumar, S.; Dang, T. D.; Arnold, F. E.; Bhattacharyya, A.R., Min, B. G., Zhang, X. F., Vaia, RA, Park, C.; Adams, W. W.; Hauge, R. H.; Smalley, R. E.; Ramesh, S.; Willis, P. A. *Macromolecules* **2002,** *35*, 9039.
5. Sreekumar, T. V.; Liu, T.; Min, B. G.; Guo, H.; Kumar, S.; Hauge, R. H.; Smalley, R. E. *Adv. Mater.* **2004,** *16*, 58.
6. Park, C.; Ounaies, Z.; Watson, K. A.; Crooks, R. E.; Smith, J.; Lowther, S. E.; Connell, J. W.; Siochi, E. J.; Harrison, J. S.; Clair, T. L. *Chem. Phys. Lett.* **2002,** *364*, 303.
7. Matarredona, O.; Rhoads, H.; Li, Z.; Harwell, J. H.; Balzano, L.; Resasco, D. E. *J. Phys. Chem. B* **2003,** *107*, 13357.
8. Moore, V. C.; Strano, M. S.; Haroz, E. H.; Hauge, R. H.; Smalley, R. E.; Schmidt, J.; Talmon Y. *Nano. Lett.* **2003,** *3*, 1379.
9. O'Connell, M. J.; Boul, P.; Ericson, L. M.; Huffman, C.; Wang, Y. H.; Haroz, E.; Kuper, C.; Tour, J.; Ausman, K. D.; Smalley, R. E. *Chem. Phys. Lett.* **2001,** *342*, 265.
10. Zhang, X. F.; Liu, T.; Sreekumar, T. V.; Kumar, S.; Moore, V. C.; Hauge, R. H.; Smalley, R. E. *Nano. Lett.* **2003,** *3*, 1285.
11. Lin, Y.; Zhou, B.; Fernando, K. A. S.; Liu, P.; Allard, L. F.; Sun, Y. P. *Macromolecules* **2003,** *36*, 7199.
12. Paiva, M. C.; Zhou, B.; Fernando K. A. S.; Lin, Y.; Kennedy, J. M.; Sun, Y. P. *Carbon* **2004,** *42*, 2849.
13. Ajayan, P. M.; Stephen, O.; Colliex, C.; Trauth, D. *Science* **1994,** *265*, 1212.
14. Minus, M. L.; Chae, H. G.; Kumar, S. *Polymer* **2006,** *47*, 3705.
15. Kimura, T.; Ago, H.; Tobita, M.; Ohshima, S.; Kyotani, M.; Yumura, M. *Adv. Mater.* **2002,** *14*, 1380.
16. Choi, E. S.; Brooks, J. S.; Eaton, D. L.; Al-Haik, M. S.; Hussaini, M. Y.; Garmestani, H.; Li, D.; Dahmen, K. *J. Appl. Phys.* **2003,** *94*, 6034.
17. Miaudet, P.; Badaire, S.; Maugey, M.; Derré, A.; Pichot, V.; Launois, P.; Poulin, P.; Zakri, C. *Nano. Lett.* **2005,** *5*, 2212.
18. Pichot, V.; Badaire, S; Albouy, P. A.; Zakri, C.; Poulin, P.; Launois, P. *Phys. Rev. B* **2006,** *74*, 245416.
19. Miaudet, P.; Badaire, S.; Maugey, M.; Derre, A.; Pichot, V.; Launois, P.; Poulin, P.; Zakri, C. *Nano. Lett.* **2005,** *5*, 2212.
20. Vigolo, B.; Pénicaud, A.; Coulon, C.; Sauder, C.; Pailler, R.; Journet, C.; Bernier, P.; Poulin, P. *Science* **2000,** *290*, 1331.
21. Dalton, A. B.; Collins, S.; Muñoz, E.; Ebron, V. H.; Ferraris, J. P.; Coleman, J. N.; Kim, B. G.; Baughman, R. H. *Nature* **2003,** *423*, 703.
22. Zhang, X. F.; Liu, T.; Sreekumar, T. V.; Kumar, S.; Hu, X. D.; Smith, K. *Polymer* **2004,** *45*, 8801.
23. Xu, X.; Uddin, A. J.; Aoki, K.; Gotoh, Y.; Saito, T.; Yumura, M. *Carbon* **2010,** *48*, 1977.
24. Minus, M. L., Chae, H. G.; Kumar, S. *Macromol. Chem. Phys.* **2009,** *210*, 1799.
25. Naebe, M.; Lin, T.; Tian, W.; Dai, L.; Wang, X. *Nanotechnology* **2007,** *18*, 225605.
26. Hu, H.; Bhowmik, P.; Zhao, B.; Hamon, M. A.; Itkis, M. E.; Haddon, R. C. *Chem. Phys. Lett.* **2001,** *345*, 25.
27. Shao, C. L.; Yu, N.; Liu, Y. C.; Mu, R. X.; *J. Phys. Chem. Solids* **2006,** *67*, 1423.
28. Sreedhar, B.; Sairam, M.; Chattopadhyay, D. K.; Rathnam, P. A. S.; Rao, D. V. M.; *J. Appl. Polym. Sci.* **2005,** *96*, 1313.
29. Keller, A. *Faraday Discuss. Chem. Soc.* **1979,** *68*, 145.
30. Jorio, A.; Pimenta, M. A.; Souza, F. A. G.; Saito, R.; Dresselhaus, G.; Dresselhaus, M. S. *New J. Phys.* **2003,** *5*, 139.1.
31. Fischer, D.; Petra, P.; Harald, B.; Andreas, J. *Macromol. Symp.* **2005,** *230*, 167.